ANNALS of Faculty Engineering Hunedoara
– International Journal of Engineering
Tome XIII [2015] – Fascicule 4 [November]
ISSN: 1584-2673 [CD-Rom; online]
a free-access multidisciplinary publication of the Faculty of Engineering Hunedoara

[1.] Horea HORA, [2.] Cristina HORA, [3.] Simona DZIȚAC

MODELING AND SIMULATION OF AN OPTO-MECHANICAL SYSTEM USING FEM

[1-3.] University of Oradea, Faculty of Managerial and Technological Engineering, Faculty of Power Engineering, Oradea, ROMANIA

Abstract: The paper presents a detailed study of the mechanical stress effect on the optical components in their ideal, nominal positioning relation to an optical or a geometric axis of an opto - mechanical subassembly. The object of analysis is an achromatic doublet limited to diffraction, an original concept. Its modeling and the simulation of mechanical part effects are made using Abaqus finite element program. Through the processing digital data from Abaqus and taken over in Microsoft Excel have been determined the real and deformed generators of diopter lens on the analytical canonical forms. The results of the analysis for multiple load cases allow the birefringence phenomenon occurrence and evolution study as well as its correlation with the size of the additional strains of wave front.
Keywords: Lenses, stress and strain, Finite Element Method (FEM), Abaqus software

1. INTRODUCTION

An optical system of the highest quality, limited to diffraction, may be affected by design faults of optical or mechanical parts and by assembly errors. Optical systems alignment is a fundamental condition for image quality [10], and as a result, the relative positions of optical components and optical subassemblies gain a special importance compared to mechanical mounts and require more careful monitoring than in other technical applications.

To achieve a meaningful analysis of optical components stress and strain, in order to highlight the influence of mechanical stress on image quality we proceeded to design an achromated doublet [1], [2], [3], [7], [9], representative for optical systems. A pair of compatible materials commonly used was chosen (BK7, SF 5, Schott catalog), a Fraunhofer constructive solution (converging lens or crown glass at the front) and standard reference features (f '= 100 mm, an opening number f / 7 aperture, item 5 ° field angle).

2. ANALYSIS OF AN OPTO–MECHANICAL SYSTEM MODEL IN ABAQUS PROGRAM BASED ON AUTOCAD GENERATED STRUCTURE

The doublet's geometry, obtained through a synthesis based on optical algorithms, was converted into a numerical model, stored in a vector graphics file. The subassembly's draft contains 3D representations of the components. A meridian section (flat and axonometric), containing converging lens (red), diverging lens (blue), screw ring (green) and the mount (gray) is shown in figure 1.

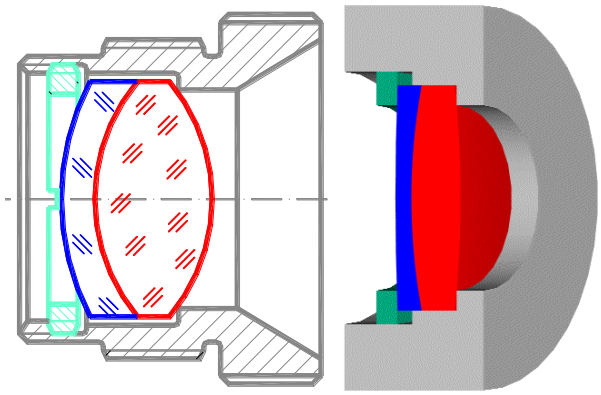

Figure 1 – The CAD meridian section of an opto - mechanical subassembly made up of doublet, threaded ring and mount

The two lenses were saved as AutoCAD solid models generated with the extension * .sat which is compatible with the filters of Abaqus [4], [5], [9], graphics import module. The two lenses, converging and diverging were declared distinct parts, which were assigned initial properties of homogeneity and isotropy, elastic behavior characterized by constants: $E=8.2\cdot10^7$ MPa, $\nu=0.206$ (for BK7 type) and $E=5.6\cdot10^7$ MPa, $\nu=0.233$ (for SF 5 type). Optical stress coefficients have the values $k=2.77\cdot10^{-6}$ mm^2/N, respectively $k=2.99\cdot10^{-6}$ mm^2/N.

The 3D solid model in axonometric representation, respectively a side view of the doublet in wireframe style meshed with tetrahedral elements are shown in figure 2. Compressing strain of threaded ring was modeled, applying constant pressure on the contact surface of diverging lens - threaded ring. As a numerical value contact pressure was considered relevant and not the normal contact force or torque screw ring.

Program runs for pressure values p = 2 MPa, 5 MPa and 10MPa were realized.

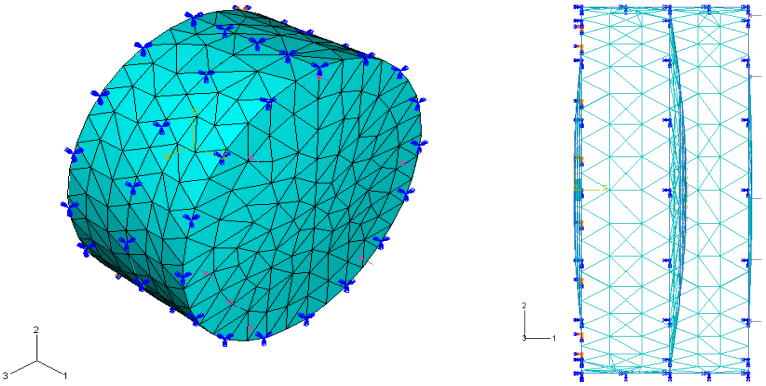

Figure 2 – The 3D solid and wireframe model of the doublet highlighting the mesh in tetrahedral elements

□ contact pressure p = 2 MPa

Figures 3 and 4 shows the variation of the von Mises stresses [4], [5], in representation of deformed structure so as to highlight the converging lens (Figure 3) and the diverging lens (Figure 4). Imported graphic files contain chromatic scales, which, conventionally, from red to blue, indicate stress in a descending order.

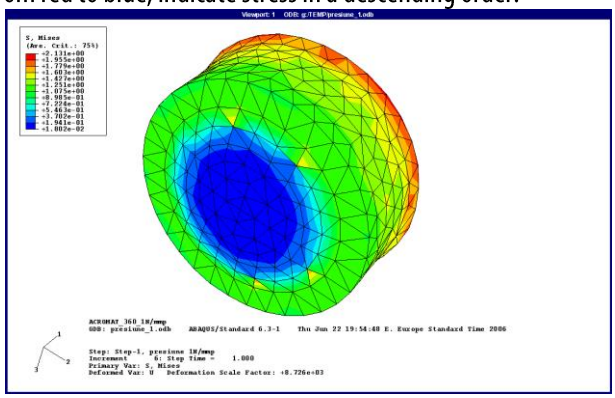

Figure 3 - The von Mises stresses variation for converging lens

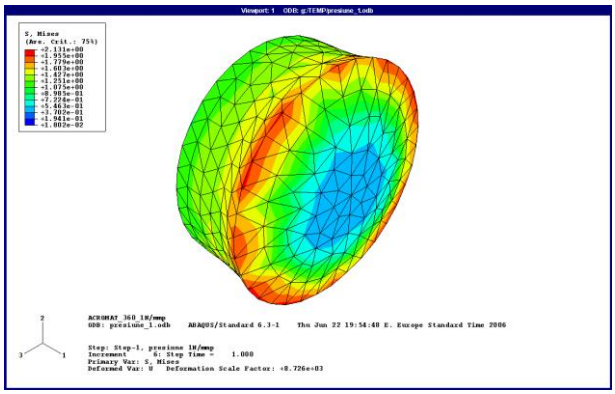

Figure 4 - The von Mises stresses variation for diverging lens

It is noted that the maximum stress are obtained next to the contact area of the diverging lens. Stress variation for the converging lens has the same rate, noting that the maximum values related to mount contact are only half of those of the diverging lens.

The deformed structure study shows that the assembly operation lead to a compression in the marginal area and an extension in the center of both lenses, mainly parallel to the optical axis. This observation is confirmed by σ_x component variation illustrated in figure 5 for the converging lens and in figure 6 for the diverging lens. These stress have approximate maximum values equal to the applied pressure.

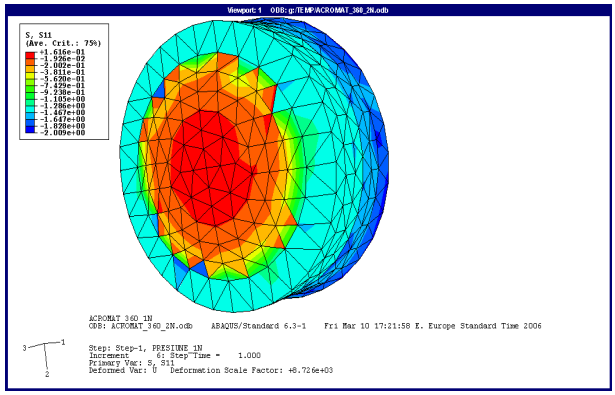

Figure 5 – The σ_x variation for the converging lens

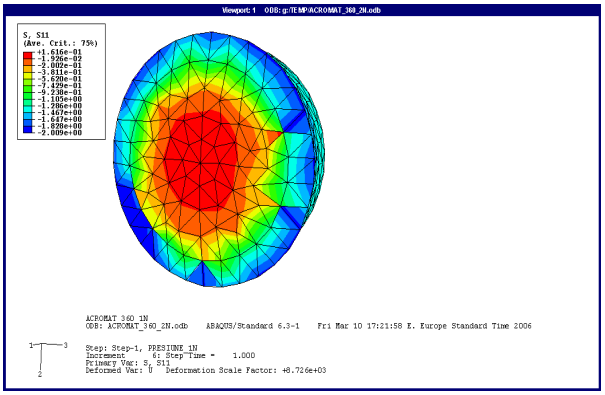

Figure 6 - The σ_x variation for the diverging lens

In order to highlight the converging lens spherical surface deformation a set of nodes belonging to a partition meridian plan was created. Numerical data for these nodes are shown in table 1.

The serial numbers of nodes are those of the automatic generation of the structure. Columns 1, 2 and 3 show the initial node coordinate values (direction x-parallel to the optical axis), the movement in the x direction and the node coordinate on deformed generator. The last column shows the initial radius corresponding to the nominal spherical surface.

Table 2 shows Y coordinates of the initial surface, respectively the deformed surface.

Table 1. Numerical data

ID NOD	X_0	ΔX_{2MPa}	X_{2MPa}	r_{CERC}
0	1	2	3	4
9	4.28578E-01	0.00000E+00	4.28578E-01	62.00
6	2.97308E-01	-3.26300E-05	2.97275E-01	62.00
7	1.90112E-01	-4.35500E-05	1.90068E-01	62.00
32	1.06866E-01	-4.79900E-05	1.06818E-01	62.00
30	4.74734E-02	-4.98700E-05	4.74235E-02	62.00
3	1.18649E-02	-5.01800E-05	1.18147E-02	62.00
1	0.00000E+00	-5.04750E-05	-5.04750E-05	62.00
2	1.18649E-02	-5.01500E-05	1.18148E-02	62.00
29	4.74734E-02	-4.95600E-05	4.74238E-02	62.00
31	1.06866E-01	-4.76300E-05	1.06818E-01	62.00
4	1.90112E-01	-4.32800E-05	1.90069E-01	62.00
5	2.97308E-01	-3.23300E-05	2.97276E-01	62.00
8	4.28578E-01	0.00000E+00	4.28578E-01	62.00

Table 2. Coordinates of the initial surface and the deformed surface

ID NOD	Y_0	ΔY_{2MPa}	Y_{2MPa}
0	1	2	3
9	7.27736E+00	0.00000E+00	7.27736E+00
6	6.06477E+00	5.72200E-06	6.06478E+00
7	4.85157E+00	-4.29100E-06	4.85157E+00
32	3.63868E+00	-1.90700E-06	3.63868E+00
30	2.42579E+00	7.15200E-07	2.42579E+00
3	1.21289E+00	1.19200E-07	1.21289E+00
1	0.00000E+00	-8.68400E-08	-8.68400E-08
2	-1.21289E+00	-3.57600E-07	-1.21289E+00
29	-2.42579E+00	-7.15200E-07	-2.42579E+00
31	-3.63868E+00	-2.14500E-06	-3.63868E+00
4	-4.85157E+00	-4.76800E-06	-4.85157E+00
5	-6.06447E+00	-7.15200E-06	-6.06448E+00
8	-7.27736E+00	0.00000E+00	-7.27736E+00

It is noted that the movements in this case have values small enough to be considered insignificant. Determination of aspheric generator quadric curve constant was done using general equation of quadric curves:

$$x = \frac{y^2 cv}{1+\sqrt{1-y^2 cv^2 (k+1)}} \tag{1}$$

where cv represents the inverse of the diopter's nominal radius, k – quadric curve constant.
The analytical equation of the deformed diopter is:

$$x = \frac{y^2}{62\left(1+\sqrt{1-\frac{0.31y^2}{62^2}}\right)} \tag{2}$$

The deformed surface is represented in figure 7.

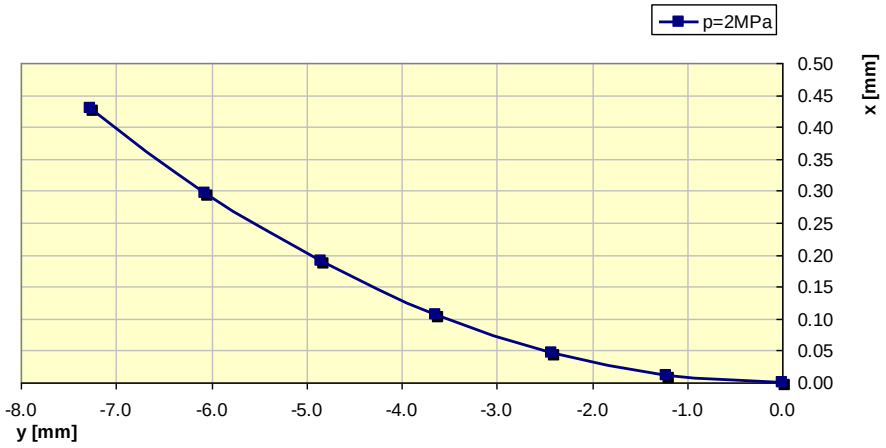

Figure 7 – The generating curve of the converging lens deformed surface

Because of the geometric and load symmetry the displacements on Z axis' direction are insignificant (10^{-8} ... 10^{-9} order).
Similarly, tables 3 and 4 contain data referring to initial and final coordinates of the diverging lens free diopter.

Table 3. Initial coordinates

ID NOD	X_0	ΔX_{2MPa}	X_{2MPA}	r_{CERC}
0	1	2	3	0
19	9.30205E+00	-1.46800E-04	9.30190E+00	128.10
99	9.39000E+00	-7.62900E-05	9.38992E+00	128.09
16	9.45620E+00	-5.14900E-05	9.45615E+00	128.09
92	9.48800E+00	-4.67300E-05	9.48795E+00	128.09
17	9.50000E+00	-4.38600E-05	9.49996E+00	128.09
93	9.47812E+00	-4.67300E-05	9.47807E+00	128.08
18	9.45624E+00	-5.24500E-05	9.45619E+00	128.09
100	9.37915E+00	-7.43800E-05	9.37908E+00	128.08
20	9.30205E+00	-1.49700E-04	9.30190E+00	128.10

Table 4. Final coordinates

ID NOD	Y_0	ΔY_{2MPa}	Y_{2MPa}
0	1	2	3
19	7.27736E+00	5.43500E-05	7.27741E+00
99	5.31264E+00	4.43400E-05	5.31268E+00
16	3.34792E+00	2.52700E-05	3.34795E+00
92	1.67396E+00	1.12000E-05	1.67397E+00
17	0.00000E+00	1.92300E-07	1.92300E-07
93	-1.67396E+00	-1.04900E-05	-1.67397E+00
18	-3.34792E+00	-2.38400E-05	-3.34794E+00
100	-5.31264E+00	-4.19600E-05	-5.31268E+00
20	-7.27735E+00	-5.53100E-05	-7.27741E+00

Analyzing the two tables it is noted that the same observations as for the converging lens are valid.
Figure 8 shows the aspherical generator of the the divergent lens free diopter.

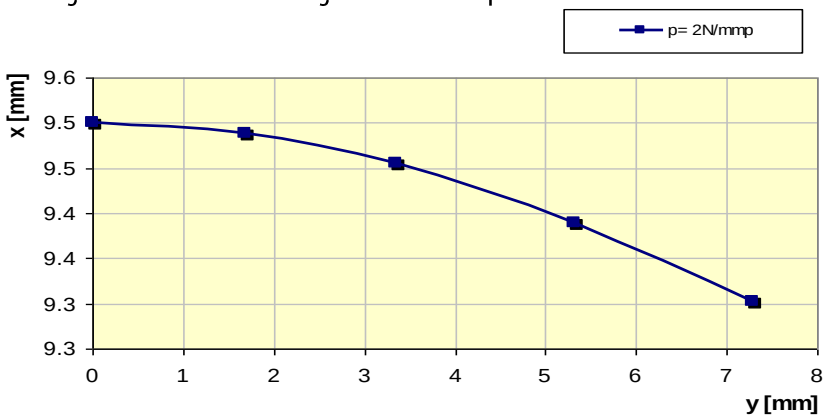

Figure 8 – The generating curve of the diverging lens deformed surface

The quadric curve constant amounting to -0.43 also indicates a deformation of the initial circle, which turns into an ellipse.
The analytical equation of the deformed diopter is:

$$x = \frac{1}{-128.1} \cdot \frac{y^2}{\left(1+\sqrt{1-\frac{0.57y^2}{128.1^2}}\right)} \qquad (3)$$

❒ **contact pressure 5 Mpa** [6]

In figure 9 is presented von Mises stresses variation.

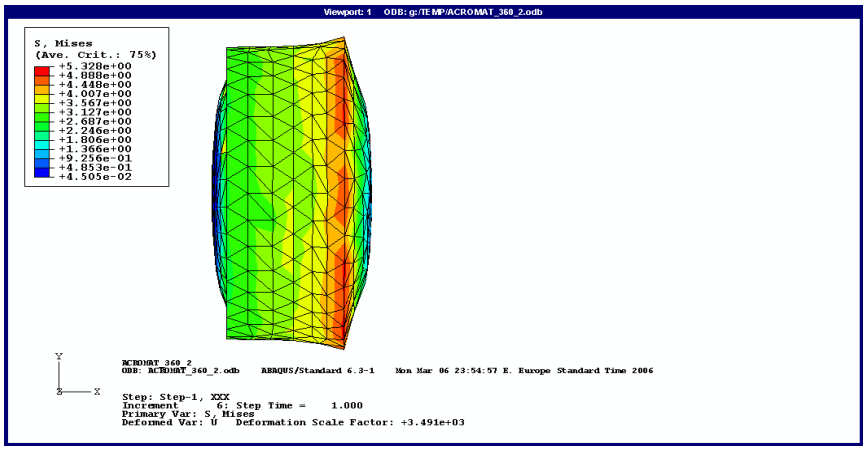

Figure 9 – The von Mises stresses variation for p = 5 MPa

It is noted that the equivalent stress are substantially equal to the applied pressure and have a variation similar to that described for the previous case. Deformations are also qualitatively similar.

The most important component of normal stress is X-axis oriented. For diverging lens, the maximum value $\sigma_x \cong p$ and for converging lens $\sigma_x \cong p/2$ (figures 10 and 11).

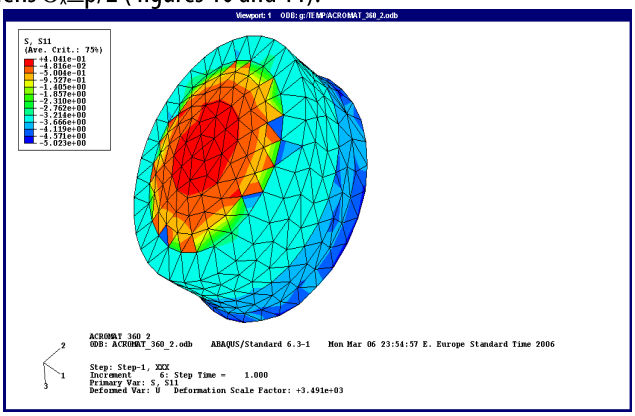

Figure 10 – The σ_x variation for the converging lens

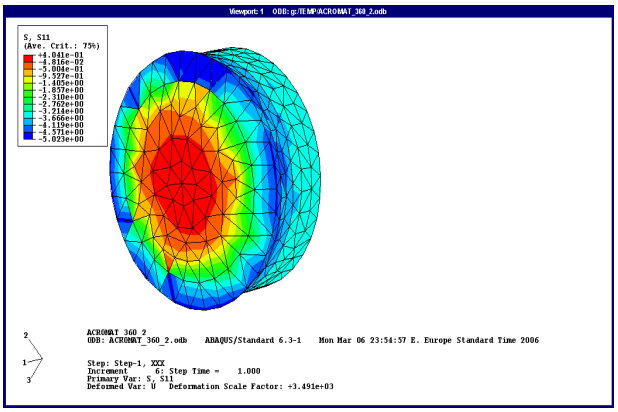

Figure 11 - The σ_x variation for the diverging lens

Based on coordinates X, Y – initial and final - of nodes belonging to the generators of the lenses free dioper are obtained the generating curve of the converging / diverging lens deformed surface (figures 12 and 13).

❒ **contact pressure p=10MPa** [6]

The same elements of analysis were taken for a load of p = 10MPa. The conclusions are qualitatively similar to those above. Numerical analysis reveals an increase of stress and strains, respectively quadric curve constants.

The generating curves of the converging / diverging lens deformed surface are presented in figures 14 and 15.

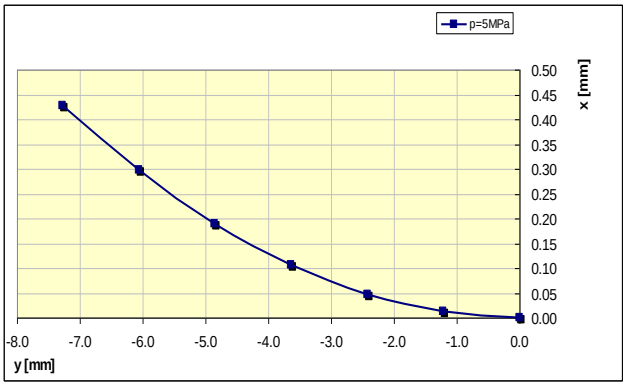

Figure 12 - The elliptical generating curve of the converging lens

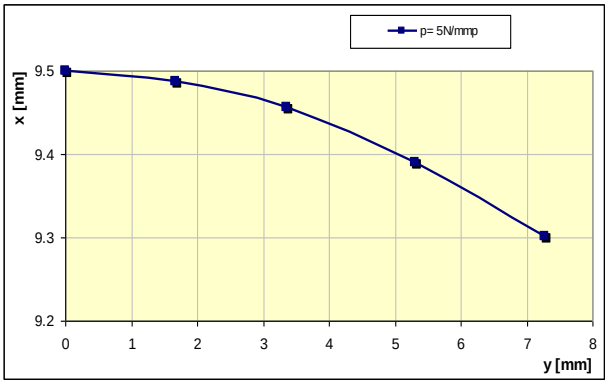

Figure 13 - The elliptical generating curve of the diverging lens

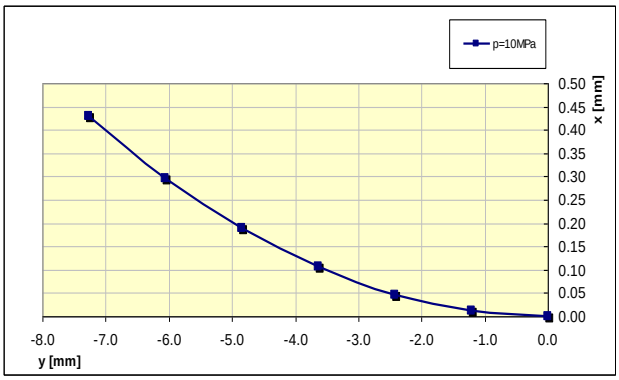

Figure 14 - The generating curve of the converging lens

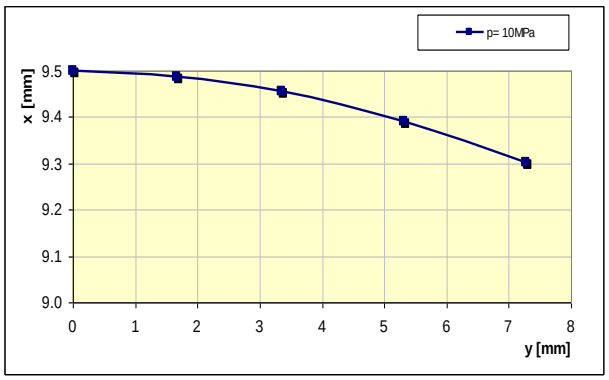

Figure 15 - The generating curve of the diverging lens

3. CONCLUSIONS:

≡ even if the nominal position of the optical subassembly in the mount is maintained, practicing an incorrect connection with uncontrolled pressing of the lens between mount and screw ring can lead to the image depreciation.

≡ tension and deformation of the lens leads to birefringence and deformation of the diopter that can be seen as a deviation from nominal spherical shape.

≡ maximum equivalent von Mises stresses are approximately equal to the loading of the lens on which the external load is directly applied and halved values for the following optical piece. It follows that for a complex optical system, consisting of a longer series of lenses, the most affected is that which comes into direct contact with the threaded ring. Pressure effect diminishes significantly on the following components.

≡ stress and strain for optical components has special significance to the characteristic approach of machine in general. The stresses have small absolute values, which are not rational subject to sizing or verification operations. Optical glass has a very high resistance to compression, so the danger of damage due to this application doesn't exist. But stresses presence, even at very low values, can induce the birefringence phenomenon, which affects seriously the image quality.

References

[1.] Gruescu, C., Strauți Negru, G., Nicoara I., Aspects concerning the influence of execution errors of optical components upon the image quality, the VIth international Conference on Precison Mechanics and Mechatronics COMEFIM-6, Brasov, 2002, volume 1-20a, p 281-284

[2.] Gruescu, C., Nicoară, I., The cemented achromat – a critical view, Politechnica Timişoara Publishing, Tom 45(59), Mechanical serie, 1999

[3.] Gruescu., C. Nicoară, I., Optical devices. Analysis and synthesis of optical lenticular systems. Politechnica Timişoara Publishing 2004, ISNB 973-625-158-6

[4.] Hora H., Hora C., The Finite Element Method Used for Analysis the Triaxial Stress and Strain State, Annals of the Oradea University, Fascicle of Management and Technological Engineering, volume XXIII(XIII), No. 3, 2014, ISSN 1583-0691

[5.] Hora H., Hora C., - Abaqus Used in Solving Elasticity Problems of Lens Mounts, Annals of the Oradea University, Fascicle of Management and Technological Engineering, volume XXIII(XIII), No. 3, 2014, ISSN 1583-0691

[6.] Hora H., Contributions to stress and strain influence of opto – mechanical systems on image quality, Politechnica Timişoara Publishing, 2009, ISSN 1842-4937, ISBN 978-973-625-880-0

[7.] Kingslake, R., Lens design fundamentals, Academic Press, N.Y.,1978

[8.] Shannon, R.R., Optical Specification, in Handbook of Optics, vol.I, ch.34, McGraw Hill Inc., NY,1995

[9.] Okruhlik, M., Finite Element Homework and Programming Applications, IFToM, p. 3161-3165, Politehnica di Milano, 1995

[10.] O'Shea, D.C., Harrigan, E., Aberration Curves in Lens Design, in Handbook of Optics, vol.I, ch. 33, McGraw Hill Inc., NY,1995

ANNALS of Faculty Engineering Hunedoara – International Journal of Engineering